

Vortex rings in heavy-ion collisions at energies $\sqrt{s_{NN}} = 3\text{--}30$ GeV and possibility of their observation

Yu. B. Ivanov^{1,2,3,*}

¹*Bogoliubov Laboratory of Theoretical Physics, JINR, Dubna 141980, Russia*

²*National Research Nuclear University "MEPhI", Moscow 115409, Russia*

³*National Research Center "Kurchatov Institute", Moscow 123182, Russia*

The ring structures that appear in Au+Au collisions at collision energies $\sqrt{s_{NN}} = 3\text{--}30$ GeV are studied. The calculations are performed within the model of three-fluid dynamics. It is demonstrated that a pair of vortex rings are formed, one at forward and another at backward rapidities, in ultra-central Au+Au collisions at $\sqrt{s_{NN}} > 4$ GeV. The vortex rings carry information about early stage of the collision, in particular about the stopping of baryons. It is shown that these rings can be detected by measuring the ring observable R_Λ even in rapidity range $0 < y < 0.5$ (or $-0.5 < y < 0$) on the level of 0.5–1.5% at $\sqrt{s_{NN}} = 5\text{--}20$ GeV. At forward/backward rapidities, the R_Λ signal is expected to be stronger. Possibility of observation of the vortex-ring signal against background of non-collective transverse polarization is discussed.

PACS numbers: 25.75.-q, 25.75.Nq, 24.10.Nz

Keywords: relativistic heavy-ion collisions, hydrodynamics, polarization

I. INTRODUCTION

Vortex rings are inherent in fluid dynamics. They are developed in a cylindrically symmetric flow of fluid with the longitudinal velocity depending on the radius. Such flow results in formation of toroidal vorticity structures, i.e. the vortex rings. An example of such vortex rings is the smoke rings.

Formation of vortex rings in heavy ion collisions at high collision energies, $\sqrt{s_{NN}} = 40\text{--}200$ GeV, was predicted in hydrodynamic [1] and transport [2, 3] simulations. Later, the vortex rings were reported at lower energy of 7.7 GeV in simulations in Refs. [4, 5]. Earlier, ring-like structures, i.e. half rings, were noticed in semi-central Au+Au collisions at even lower energy of 5 GeV [6, 7]. The authors of Refs. [6, 7] called this specific toroidal structure as a femto-vortex sheet. In recent paper [8], formation of the vortex rings was predicted in Au+Au collisions at $\sqrt{s_{NN}} = 7.7\text{--}11.5$ GeV and even at 4.5 GeV, where the ring structure turns out to be more diffuse.

Formation of vortex rings is a consequence of partial transparency of colliding nuclei at high energies. The matter in the central region is more strongly decelerated because of thicker matter in the center than that at the periphery. Therefore, two vortex rings are formed at the periphery of the stronger stopped matter in the central region, one at forward rapidities and another at backward rapidities. The peripheral matter acquires a rotational motion. Matter rotation is opposite in these two rings. A schematic picture of the vortex rings is presented in Fig. 1.

The partial transparency takes place at the early stage of the collision, even before equilibration of the produced matter. It determines the strength of vorticity in the vor-

tex rings. Therefore, the vortex rings carry information about this early stage of the collision.

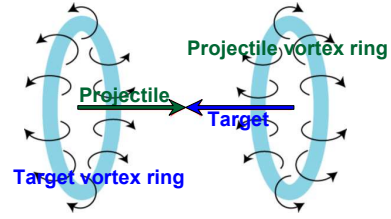


FIG. 1: (Color online) Schematic picture of the vortex rings at forward/backward rapidities. Curled arrows indicate direction of circulation of the matter.

In Ref. [9], the analysis of the toroidal vortex structures was extended to proton-nucleus collisions. It was predicted that vortex rings are created in such collisions at the energy of $\sqrt{s_{NN}} = 200$ GeV. Vortex rings produced by jets propagating through the quark-gluon matter were considered in Ref. [10]. The above predictions [1–10] were obtained within different models. Thus, it looks like the vortex rings are quite common for the high-energy nucleus(proton)-nucleus collisions. The question is how to observe them.

Authors of Refs. [9, 10] suggested a ring observable

$$R_\Lambda(y) = \left\langle \frac{\mathbf{P}_\Lambda \cdot (\mathbf{e}_z \times \mathbf{p})}{|\mathbf{e}_z \times \mathbf{p}|} \right\rangle_y, \quad (1)$$

where $\mathbf{P}_\Lambda(\mathbf{p})$ is the polarization of the Λ hyperon, \mathbf{p} is its spacial momentum, and \mathbf{e}_z is the unit vector along the beam, i.e. along z axis. Averaging $\langle \dots \rangle_y$ runs over all momenta with fixed rapidity y . As argued in Ref. [9, 10], the ring structure may be quantified by means of R_Λ .

However, the same ring observable turns out to be nonzero in proton-proton and proton-nucleus collisions, see, e.g., Refs. [11, 12] where a brief survey of earlier experiments is also presented. It is referred as a transverse

*e-mail: yivanov@theor.jinr.ru

polarization in those experiments. At least in proton-proton reactions, the nonzero R_Λ is related to the correlation of the produced Λ with beam direction rather than to the collective ring structure. To be precise, only the collective contribution to R_Λ due to the vortex rings are estimated below while the discussion of the background of direct Λ production is postponed to the end of the paper.

This ring observable was applied to analysis of ultra-central Au+Au collisions at $\sqrt{s_{NN}} = 200$ GeV [9]. It was found that nonzero values of R_Λ appear only at rapidities $|y| > 4$, i.e. far beyond the midrapidity window accessible in collider experiments. Therefore, questions arise:

- (i) whether the vortex rings can be observed at lower-energy collider experiments at BES RHIC (Beam Energy Scan program at the Relativistic Heavy Ion Collider) and NICA (Nuclotron-based Ion Collider fAcility) within the experimental midrapidity window and
- (ii) whether the vortex rings are formed in lower-energy collisions of the STAR fixed-target program (FXT-STAR) at RHIC the forthcoming experiments at the Facility for Antiproton and Ion Research (FAIR), where measurements at backward rapidities are possible?

In the present paper, the ring structures in Au+Au collisions at collision energies $\sqrt{s_{NN}} = 3\text{--}30$ GeV are studied and the resulting ring observable is estimated. The calculations are performed within the model of the three-fluid dynamics (3FD) [13]. The 3FD approximation is a minimal way to simulate the early, nonequilibrium stage of the produced strongly interacting matter. It takes into account counterstreaming of the leading baryon-rich matter at the early stage of nuclear collisions. This counterstreaming results in formation of the vortex rings.

The simulations are done with two different equations of state (EoS's): two versions of the EoS with the deconfinement transition [14], i.e. a first-order phase transition (1PT) and a crossover one. The physical input of the present 3FD calculations is described in Ref. [15].

II. VORTICAL RINGS IN CENTRAL COLLISIONS

The particle polarization is treated within the thermodynamic approach [16], in which it is related to the thermal vorticity

$$\varpi_{\mu\nu} = \frac{1}{2}(\partial_\nu\beta_\mu - \partial_\mu\beta_\nu), \quad (2)$$

where $\beta_\mu = u_\mu/T$ with u_μ and T being the local collective velocity of the matter and its temperature, respectively. The thermal vorticity is directly related to the mean spin vector of spin 1/2 particles with four-momentum p , produced around point x on freeze-out hypersurface

$$S^\mu(x, p) = \frac{1}{8m}[1 - n_F(x, p)] p_\sigma \epsilon^{\mu\nu\rho\sigma} \varpi_{\rho\nu}(x), \quad (3)$$

where $n_F(x, p)$ is the Fermi-Dirac distribution function and m is mass of the considered particle. The polarization vector of S -spin particle is defined as $P_S^\mu = S^\mu/S$. The polarization of the Λ hyperon is measured in its rest frame, therefore the Λ polarization should be additionally boosted to the Λ rest frame.

Let us first consider the structure of the thermal-vorticity field in heavy-ion collisions in the $x\eta_s$ plane, where $\eta_s = (1/2)\ln[(t+z)/(t-z)]$ is the longitudinal space-time rapidity and z is the coordinate along the beam direction. The advantage of this η_s is that it is equal to the kinematic longitudinal rapidity defined in terms of the particle momenta in the self-similar one-dimensional expansion of the system.

The plot of ϖ_{zx} in ultra-central ($b = 0$ fm) Au+Au collisions at $\sqrt{s_{NN}} = 4.9\text{--}11.5$ GeV in the $x\eta_s$ plane is presented in Fig. 2. In order to suppress contributions of almost empty regions, the displayed thermal-vorticity ϖ_{zx} is averaged with the weight of proper energy density (also presented in Fig. 2) similarly to that in Refs. [1, 4]. The $x\eta_s$ plane would be a reaction plane in case of non-central collisions. In our case ($b = 0$ fm), all the planes passing through the z axis are equivalent because of the axial symmetry. These are the plots at time instants close to the freeze-out. In order to see correlations of the thermal-vorticity with other quantities, plots of the proper energy density, kinematic zx vorticity

$$\omega_{\mu\nu} = (1/2)(\partial_\nu u_\mu - \partial_\mu u_\nu),$$

divided by temperature, x -component of the baryon current (J_x) and the proper baryon density are also displayed.

As seen, the thermal-vorticity reveals a ring structure similar to that schematically displayed in Fig. 1. The $x\eta_s$ plane is a cut of these rings by the plane passing through the axis of these rings. This ring structure is seen even at $\sqrt{s_{NN}} = 4.9$ GeV. The kinematic zx vorticity (the third column of panels in Fig. 2) reveals the same ring structure. This indicates that these rings are due to the incomplete stopping of the peripheral parts of the colliding nuclei. If the rings were formed as a result of the hydrodynamic quasi-one-dimensional expansion of initially stopped matter, then the sign of ω_{zx}/T would be opposite because the longitudinal flow velocity would decrease from the center of the flow to its periphery, as in the case of high-energy proton-nucleus collisions [9]. Comparing the scales of ϖ_{zx} and ω_{zx}/T in Fig. 2, we see that approximately half of the magnitude of the thermal vorticity results from derivatives of the inverse temperature.

As seen from Fig. 2, these thermal-vorticity rings correlate with transverse component of the baryon current (J_x). It means that the vortical rings expand, which is important for their observation. At the same time, the proper energy and density distributions reveal a disk rather than ring structure although at the same space-time rapidities. At 4.9 GeV, this is already a central fireball rather than two disks.

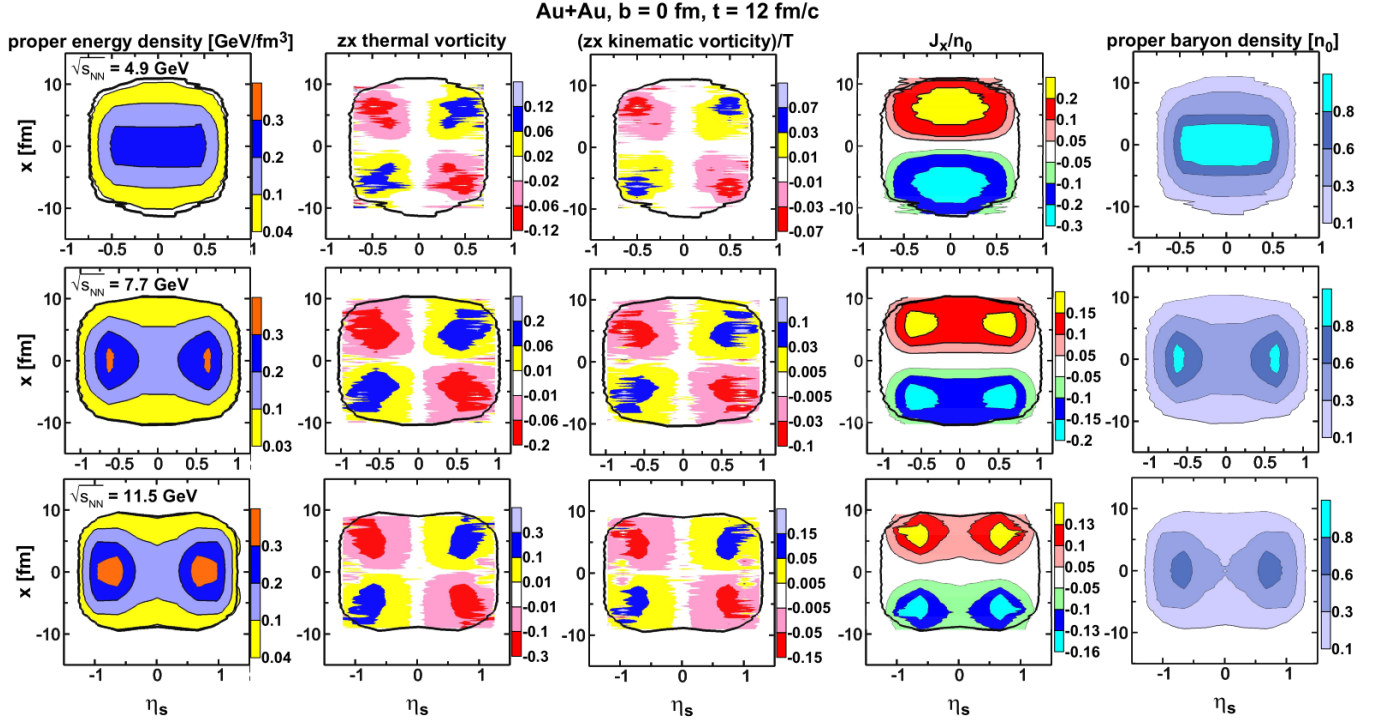


FIG. 2: (Color online) Columns from left to right: the proper energy density (GeV/fm^3), the proper-energy-density weighted thermal zx vorticity, similarly weighted kinematic zx vorticity divided by temperature (T), x -component of the baryon current (J_x) in units of normal nuclear density ($n_0 = 0.15 \text{ 1}/\text{fm}^3$), and the proper baryon density (n_B) in units of n_0 in the $x\eta_s$ plane at time instant $t = 12 \text{ fm}/c$ in the ultra-central ($b = 0 \text{ fm}$) Au+Au collisions at $\sqrt{s_{NN}} = 4.9\text{--}11.5 \text{ GeV}$. η_s is the space-time rapidity along the beam (z axis) direction. Calculations are done with the crossover EoS. The bold solid contour displays the border of nuclear matter with $n_B > 0.1n_0$.

At considered moderately relativistic energies, the expansion dynamics of the system is not of the self-similar one-dimensional character. Therefore, the space-time rapidity η_s is not equal to the kinematic longitudinal rapidity in terms of the particle momenta. Nevertheless, it can be used to approximately estimate the rapidity location of these vortex rings. As seen from Fig. 2, at 4.9 GeV these rings are located slightly below $|\eta_s| = 0.5$ and at $|\eta_s| \approx 0.5$, if $\sqrt{s_{NN}} = 7.7 \text{ GeV}$. This location does not restrict their observation because the FXT-STAR experiments allow measurements at very backward rapidities. At $\sqrt{s_{NN}} = 11.5 \text{ GeV}$, where the estimation in terms of η_s is more reliable, these vortex rings are already located at $|\eta_s| \approx 0.5\text{--}1.0$, which is slightly beyond the rapidity window of the collider experiment. Nevertheless, the inner parts of these rings are still at $|\eta_s| < 0.5$. Therefore, their effect can be observed.

III. RING OBSERVABLE

To quantify the above qualitative considerations, let us turn to the ring observable of Eq. (1). Our goal is to estimate the expected ring observable in the ultra-central ($b = 0 \text{ fm}$) Au+Au collisions rather than to calculate it.

In terms of hydrodynamic quantities, the contribution

of an element of the freeze-out surface $d\Sigma_\nu$ to the ring observable reads

$$R_\Lambda(x, p) = \frac{\varepsilon^{\mu\nu\rho\sigma} P_\mu^\Lambda n_\nu e_\rho p_\sigma}{|\varepsilon^{\mu\nu\rho\sigma} n_\nu e_\rho p_\sigma|} \quad (4)$$

where $e^\sigma = (0, 0, 0, 1)$ is the unit vector along the beam (z) axis, n_ν is the normal vector to the element of the freeze-out surface. This expression coincides with Eq. (10) in Ref. [9].

To calculate the ring observable $R_\Lambda(y)$, $R_\Lambda(x, p)$ should be averaged over the whole freeze-out surface Σ and particle momenta

$$R_\Lambda(y_h) = \frac{\int (d^3p/p^0) \int_{\Sigma(y_h)} d\Sigma_\lambda p^\lambda n_\Lambda(x, p) R_\Lambda(x, p)}{\int (d^3p/p^0) \int_{\Sigma(y_h)} d\Sigma_\lambda p^\lambda n_\Lambda(x, p)}, \quad (5)$$

where n_Λ is the distribution function of Λ 's. Here the approximation has already been made: the constraint of fixed rapidity (y) imposed on the momentum integration is replaced by that of fixed hydrodynamical rapidity

$$y_h = \frac{1}{2} \ln \frac{u^0 + u^3}{u^0 - u^3}, \quad (6)$$

based on hydrodynamical 4-velocity u^μ , similarly to that in Ref. [17]. The y_h constraint is imposed on the freeze-out surface integration and is denoted as $\Sigma(y_h)$ in Eq.

(5). At moderately relativistic energies, the hydrodynamical rapidity is a more reliable approximation to the true rapidity than the space-time rapidity η_s .

Let us further proceed with approximations. Similarly to that in Ref. [17], let us use a simplified version of the freeze-out, i.e. an isochronous one that implies $n_\nu = (1, 0, 0, 0)$ and $(d^3p/p^0)d\Sigma_\lambda p^\lambda = d^3p d^3x$. The freeze-out instant is associated with time, when the energy density averaged over the central region reaches the value deduced from the conventional 3FD freeze-out. In conventional 3FD simulations, a differential, i.e. cell-by-cell, freeze-out is implemented [18].

Expression (3) for $S_\Lambda^\mu(x, p)$ is also simplified. The factor $(1 - n_\Lambda) \approx 1$ is taken because the Λ production takes place only in high-temperature regions, where Boltzmann statistics dominates. As spatial components of $\varpi_{\rho\nu}(x)$ are of the prime interest, the approximation $p_\sigma \epsilon^{\mu\nu\rho\sigma} \varpi_{\rho\nu} \approx p_0 \epsilon^{\mu\nu\rho 0} \varpi_{\rho\nu} \approx m_\Lambda \epsilon^{\mu\nu\rho 0} \varpi_{\rho\nu}$ is made. The latter approximation, $p_0 \approx m_\Lambda$, reduces $S_\Lambda^\mu(x, p)$, which is quite suitable for the purpose of upper estimate of the ring observable. The boost of $S_\Lambda^\mu(x, p)$ is neglected, which also reduces $S_\Lambda^\mu(x, p)$. After application of all these approximations, S_Λ^μ , and hence P_Λ^μ , becomes momentum independent. Therefore, the momentum averaging in Eq. (5) can be performed first, leaving P_Λ^μ beyond the scope of this averaging:

$$R_\Lambda(y_h) \approx \frac{\int_{\Sigma(y_h)} d^3x \rho_\Lambda(x) \frac{\mathbf{P}_\Lambda \cdot (\mathbf{u} \times \mathbf{e}_z)}{(\mathbf{u}_T^2 + 2T/m_\Lambda)^{1/2}}}{\int_{\Sigma(y_h)} d^3x \rho_\Lambda(x)}, \quad (7)$$

where $\rho_\Lambda(x)$ is the density of Λ 's, \mathbf{u}_T is transverse component of the fluid velocity, and T is the temperature. This expression is obtained in the non-relativistic approximation for the transverse collective motion. Indeed, at the freeze-out $T \approx 100$ MeV $\ll m_\Lambda$ and $v_T \lesssim 0.4$ at midrapidity [19]. At the forward/backward rapidities considered here, these values are even smaller. Here $(\mathbf{u}_T^2 + 2T/m_\Lambda)^{1/2}$ stands for $\langle |\mathbf{p}_T| \rangle / m_\Lambda$.

It is important that the system together with the vortex rings radially expands at the freeze-out stage. This expansion even determines the sign of R_Λ , as seen from Eq. (7). The contributions to R_Λ from particles emitted along the \mathbf{u} (more precisely, with momenta $\mathbf{p}_T \cdot \mathbf{u}_T > 0$) and in opposite to \mathbf{u} directions (i.e. $\mathbf{p}_T \cdot \mathbf{u}_T < 0$) partially cancel each other. The effect of this partial cancellation is described by the $(\mathbf{u}_T^2 + 2T/m_\Lambda)^{1/2}$ denominator in Eq. (7). This cancellation is negligible if the speed of the radial expansion is much larger than the thermal velocity of the fluid constituents.

Based on the axial symmetry of the ultra-central ($b = 0$) collisions, averaging in Eq. (7) can be restricted by the quadrant ($x > 0, z > 0$) of the “reaction” plane xz , [the ($x > 0, \eta_s > 0$) quadrant in Fig. 2], if $y_h > 0$. For negative y_h , it is ($x > 0, z < 0$) quadrant. Thus, this averaging becomes identical to that done in Ref. [17] for calculation of the global polarization but in a restricted

region, i.e. the ($x > 0, z > 0$) quadrant. The only difference is that the averaging over cells runs with additional weight $x u_x / (u_x^2 + 2T/m_\Lambda)^{1/2}$, where x takes into account that the integration runs over $r dr dz$ in cylindrical coordinates at fixed azimuthal angle.

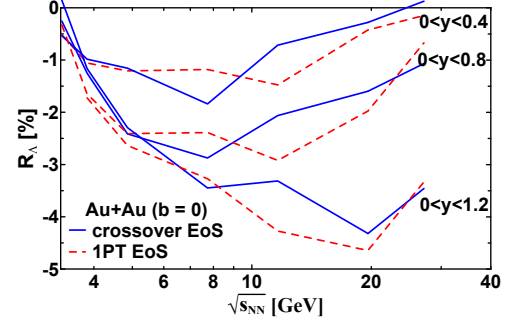


FIG. 3: (Color online) The R_Λ quantity, averaged over different rapidity ranges, in the ultra-central Au+Au collisions as function of $\sqrt{s_{NN}}$. Calculations are done with the crossover and 1PT EoS's.

The estimation of the R_Λ quantity, averaged over different rapidity ranges, in the ultra-central ($b = 0$) Au+Au collisions as function of $\sqrt{s_{NN}}$ is displayed in Fig. 3. For definiteness, all these rapidity ranges are located at positive rapidities because $R_\Lambda(y)$ is odd function of y . In fixed rapidity region, the magnitude of R_Λ first increases with the collision energy rise, reaches a maximum, the position and height of which depend on the rapidity window, and then decreases. The height of the maximum is larger in more wide rapidity windows. All these features are expected from the above qualitative consideration. The presented calculations have numerical uncertainty of 10–15%, as seen from Fig. 4 where the time dependence of the R_Λ quantity is displayed. These numerical fluctuations result from averaging over very restricted spacial region rather than the whole volume of the system, as it is done for the global polarization [17]. These fluctuations are larger for R_Λ at fixed y , also shown in Fig. 4, because the averaging runs over even more restricted spacial region in this case.

Calculations are done with the crossover and 1PT EoS's. Predictions of the different EoS's differ, but this difference is comparable with numerical uncertainty at energies below 7 GeV and above 12 GeV. However, at $7 \lesssim \sqrt{s_{NN}} \lesssim 12$ GeV this difference exceeds the numerical uncertainty. This energy range correlates with that of the earlier predicted irregularity in the excitation function of the baryon stopping [15, 20], where results of different EoS's also differ. It is not surprising because the incomplete baryon stopping (or partial transparency) is the driving forth the vortex-ring formation. In particular, this is the reason of correlation between the thermal vorticity and baryon current, see Fig. 2.

Rapidity dependence of the R_Λ quantity in the ultra-central Au+Au collisions at different $\sqrt{s_{NN}}$ is shown in Fig. 5. In view of the large numerical fluctuations, cf.

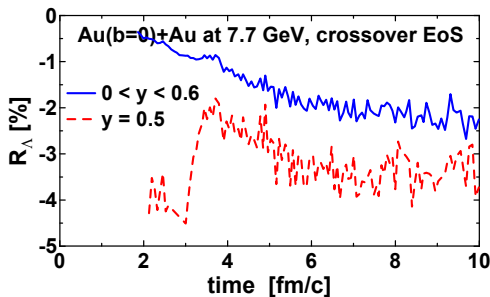


FIG. 4: (Color online) Time dependence of the R_Λ quantity, averaged over rapidity range of $0 < y < 0.6$ (solid line) and at $y = 0.5$ (dashed line), in the ultra-central ($b = 0$ fm) Au+Au collisions at $\sqrt{s_{NN}} = 7.7$ GeV. Calculations are done with the crossover EoS.

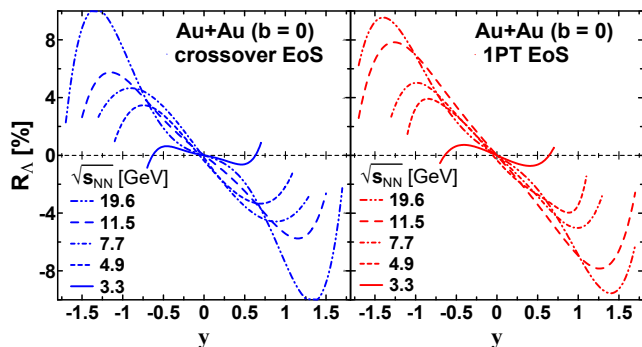


FIG. 5: (Color online) Rapidity dependence of the R_Λ quantity in the ultra-central ($b = 0$) Au+Au collisions at $\sqrt{s_{NN}} = 3.3$ –19.6 GeV. Calculations are done with the crossover (left panel) and 1PT (right panel) EoS's.

Fig. 4, the lines in Fig. 5 are smoothed by means of orthogonal-polynomial fit. Again, as expected, extreme values of R_Λ are reached at forward/backward rapidities, where the vortex rings are located. Positions of these extreme values move to larger $|y|$ with the collision energy rise. However, even at $7.7 < \sqrt{s_{NN}} < 19.6$ GeV, sizable values of R_Λ can be expected at $|y| = 0.5$ attainable in the collider mode. At lower energies, $\sqrt{s_{NN}} \leq 7.7$ GeV, measurements at backward rapidities are possible in the FXT-STAR and future FAIR experiments. At $\sqrt{s_{NN}} = 7.7$ GeV, R_Λ can reach values of 5% at backward rapidities. Feed-down from higher-lying resonances (Σ^* and Σ^0) in R_Λ has been taken into account similarly to that done for the global polarization in Ref. [17]. This feed-down reduces R_Λ by 10–15%.

IV. SUMMARY AND DISCUSSION

The ring structures that appear in Au+Au collisions at energies $\sqrt{s_{NN}} = 3 - 30$ GeV were studied, and the resulting ring observable was estimated. The calculations were performed within the 3FD model [13]. It was demonstrated that a pair of vortex rings are formed, one

at forward and another at backward rapidities, in ultra-central Au+Au collisions at $\sqrt{s_{NN}} \gtrsim 4$ GeV. The matter rotation is opposite in these two rings. They are formed because at the early stage of the collision the matter in the vicinity of the beam axis is stronger decelerated than that at the periphery. Thus, the vortex rings carry information about this early stage, in particular about the stopping of baryons.

Such 3FD dynamics with the incomplete stopping turned out to be successful in describing the global Λ polarization [17, 21], bulk [15, 22] and flow [23, 24] observables at moderately relativistic energies. Therefore, the present predictions of the vortex rings have a solid background.

These rings can be detected by measuring the ring observable R_Λ even in rapidity range $0 < y < 0.5$ (or $-0.5 < y < 0$). The R_Λ signal is stronger in wider rapidity ranges. For instance, magnitude of the ring observable may reach values of 2–3% at $\sqrt{s_{NN}} = 5$ –20 GeV, if rapidity window is extended to $0 < y < 0.8$. Measurements in fixed-target experiments, such as FXT-STAR and the forthcoming experiments at FAIR, give additional advantage. They allow measurements at backward rapidities, where the R_Λ signal is expected to be more pronounced.

Only ultra-central Au+Au collisions were considered in this paper because the axial symmetry of the system makes the R_Λ estimation easier in this case. Asymmetric vortex rings are also formed in semi-central collisions at $\sqrt{s_{NN}} > 5$ GeV. The corresponding R_Λ polarization should be asymmetric in the reaction plane.

The R_Λ quantity also contains contribution of direct Λ production with the Λ polarization correlated with beam direction. In heavy-ion collisions this type of polarization is expected to be diluted due to rescatterings in the medium [25, 26]. A vanishing Λ polarization has been proposed as a possible signature for the formation of a Quark Gluon Plasma (QGP) in relativistic heavy-ion collisions [25]. This prediction was one of motivations of the experimental study of the transverse polarization of Λ hyperons produced in Au+Au collisions (10.7A GeV) [27]. The result revealed no significant differences of the polarization from those observed in pp and pA collisions. However, the question of the nature of the obtained polarization remains open, i.e., which part of it results from the direct Λ production and which part, from to vortex rings.

Different transverse-momentum dependence may be used to distinguish these two mechanisms of the transverse polarization. While the magnitude of the transverse polarization due to the direct Λ production linearly rises with Λ transverse momentum, low- p_T Λ 's should dominate in the R_Λ due to vortex rings because these rings are collective phenomena. The p_T dependence of the vortex-ring R_Λ is expected to be decreasing, similarly to that for the global polarization [28–30]. Therefore, limiting the transverse momentum from above would enhance the contribution of the vortex rings.

Any case, the calculations of the R_Λ due to vortex rings

should be complemented by simulations of the Λ transverse polarization due to the direct Λ production, similarly to that done for the ultra-central Au+Au collisions at $\sqrt{s_{NN}} = 9$ GeV in Ref. [31]. That simulation disregarded the polarization dilution due to rescatterings in the medium. Therefore it gave the upper limit ($\approx -5\%$) on magnitude of the mean transverse Λ polarization. For the practical use, such simulations should take into account this dilution [26].

The transverse $\bar{\Lambda}$ polarization measured in pp collisions so far is consistent with zero [32]. On the other hand, the collective fluid vorticity in AA collisions polarizes all emitted particles and hence $R_\Lambda \approx R_{\bar{\Lambda}}$ should take place.

Therefore, $R_{\bar{\Lambda}}$ looks to be a good observable to detect the vortex rings.

Acknowledgments

Fruitful discussions with E. E. Kolomeitsev, O. V. Teryaev and D. N. Voskresensky are gratefully acknowledged. This work was carried out using computing resources of the federal collective usage center “Complex for simulation and data processing for mega-science facilities” at NRC “Kurchatov Institute” [33]. This work was partially supported by MEPhI within the Federal Program “Priority-2030”.

-
- [1] Y. B. Ivanov and A. A. Soldatov, “Vortex rings in fragmentation regions in heavy-ion collisions at $\sqrt{s_{NN}} = 39$ GeV,” *Phys. Rev. C* **97**, no.4, 044915 (2018) [arXiv:1803.01525 [nucl-th]].
 - [2] X. L. Xia, H. Li, Z. B. Tang and Q. Wang, “Probing vorticity structure in heavy-ion collisions by local Λ polarization,” *Phys. Rev. C* **98**, 024905 (2018) [arXiv:1803.00867 [nucl-th]].
 - [3] D. X. Wei, W. T. Deng and X. G. Huang, “Thermal vorticity and spin polarization in heavy-ion collisions,” *Phys. Rev. C* **99**, no.1, 014905 (2019) [arXiv:1810.00151 [nucl-th]].
 - [4] Y. B. Ivanov, V. D. Toneev and A. A. Soldatov, “Vorticity and Particle Polarization in Relativistic Heavy-Ion Collisions,” *Phys. Atom. Nucl.* **83**, no.2, 179-187 (2020) [arXiv:1910.01332 [nucl-th]].
 - [5] A. Zinchenko, A. Sorin, O. Teryaev and M. Baznat, “Vorticity structure and polarization of Λ hyperons in heavy-ion collisions,” *J. Phys. Conf. Ser.* **1435**, no.1, 012030 (2020).
 - [6] M. Baznat, K. Gudima, A. Sorin and O. Teryaev, “Helicity separation in Heavy-Ion Collisions,” *Phys. Rev. C* **88**, no. 6, 061901 (2013) [arXiv:1301.7003 [nucl-th]].
 - [7] M. I. Baznat, K. K. Gudima, A. S. Sorin and O. V. Teryaev, “Femto-vortex sheets and hyperon polarization in heavy-ion collisions,” *Phys. Rev. C* **93**, no. 3, 031902 (2016) [arXiv:1507.04652 [nucl-th]].
 - [8] N. S. Tsegelnik, E. E. Kolomeitsev and V. Voronyuk, “Helicity and vorticity in heavy-ion collisions at NICA energies,” arXiv:2211.09219 [nucl-th].
 - [9] M. A. Lisa, J. G. P. Barbon, D. D. Chinellato, W. M. Serenone, C. Shen, J. Takahashi and G. Torrieri, “Vortex rings from high energy central p+A collisions,” *Phys. Rev. C* **104**, no.1, 011901 (2021) [arXiv:2101.10872 [hep-ph]].
 - [10] W. M. Serenone, J. G. P. Barbon, D. D. Chinellato, M. A. Lisa, C. Shen, J. Takahashi and G. Torrieri, “ Λ polarization from thermalized jet energy,” *Phys. Lett. B* **820**, 136500 (2021) [arXiv:2102.11919 [hep-ph]].
 - [11] F. Hauenstein *et al.* [COSY-TOF], “Measurement of polarization observables of the associated strangeness production in proton proton interactions,” *Eur. Phys. J. A* **52**, no.11, 337 (2016) [arXiv:1607.06305 [nucl-ex]].
 - [12] G. Agakishiev *et al.* [HADES], “Lambda hyperon production and polarization in collisions of p(3.5 GeV)+Nb,” *Eur. Phys. J. A* **50**, 81 (2014) [arXiv:1404.3014 [nucl-ex]].
 - [13] Y. B. Ivanov, V. N. Russkikh and V. D. Toneev, “Relativistic heavy-ion collisions within 3-fluid hydrodynamics: Hadronic scenario,” *Phys. Rev. C* **73**, 044904 (2006) [arXiv:nucl-th/0503088 [nucl-th]].
 - [14] A. S. Khvorostukin, V. V. Skokov, V. D. Toneev and K. Redlich, “Lattice QCD constraints on the nuclear equation of state,” *Eur. Phys. J. C* **48**, 531-543 (2006) [arXiv:nucl-th/0605069 [nucl-th]].
 - [15] Yu. B. Ivanov, “Alternative Scenarios of Relativistic Heavy-Ion Collisions: I. Baryon Stopping,” *Phys. Rev. C* **87**, 064904 (2013) [arXiv:1302.5766 [nucl-th]].
 - [16] F. Becattini, V. Chandra, L. Del Zanna and E. Grossi, “Relativistic distribution function for particles with spin at local thermodynamical equilibrium,” *Annals Phys.* **338**, 32 (2013) [arXiv:1303.3431 [nucl-th]].
 - [17] Y. B. Ivanov and A. A. Soldatov, “Global Λ polarization in heavy-ion collisions at energies 2.4–7.7 GeV: Effect of meson-field interaction,” *Phys. Rev. C* **105**, no.3, 034915 (2022) [arXiv:2201.04527 [nucl-th]].
 - [18] V. N. Russkikh and Yu. B. Ivanov, “Dynamical freeze-out in 3-fluid hydrodynamics,” *Phys. Rev. C* **76**, 054907 (2007) [nucl-th/0611094]; Yu. B. Ivanov and V. N. Russkikh, “On freeze-out problem in relativistic hydrodynamics,” *Phys. Atom. Nucl.* **72**, 1238 (2009) [arXiv:0810.2262 [nucl-th]].
 - [19] L. Adamczyk *et al.* [STAR], “Bulk Properties of the Medium Produced in Relativistic Heavy-Ion Collisions from the Beam Energy Scan Program,” *Phys. Rev. C* **96**, no.4, 044904 (2017) [arXiv:1701.07065 [nucl-ex]].
 - [20] Y. B. Ivanov, “Baryon Stopping as a Probe of Deconfinement Onset in Relativistic Heavy-Ion Collisions,” *Phys. Lett. B* **721**, 123-130 (2013) [arXiv:1211.2579 [hep-ph]]; Y. B. Ivanov and D. Blaschke, “Robustness of the Baryon-Stopping Signal for the Onset of Deconfinement in Relativistic Heavy-Ion Collisions,” *Phys. Rev. C* **92**, no.2, 024916 (2015) [arXiv:1504.03992 [nucl-th]].
 - [21] Y. B. Ivanov, “Global Λ polarization in moderately relativistic nuclear collisions,” *Phys. Rev. C* **103**, no.3, L031903 (2021) [arXiv:2012.07597 [nucl-th]].
 - [22] Y. B. Ivanov, “Alternative Scenarios of Relativistic Heavy-Ion Collisions: II. Particle Production,” *Phys. Rev. C* **87**, no.6, 064905 (2013) [arXiv:1304.1638 [nucl-th]]; “Alternative Scenarios of Relativistic Heavy-Ion Collisions: III. Transverse Momentum Spectra,” *Phys.*

- Rev. C **89**, no.2, 024903 (2014) [arXiv:1311.0109 [nucl-th]].
- [23] Y. B. Ivanov and A. A. Soldatov, “Directed flow indicates a cross-over deconfinement transition in relativistic nuclear collisions,” Phys. Rev. C **91**, no.2, 024915 (2015) [arXiv:1412.1669 [nucl-th]].
- [24] Y. B. Ivanov and A. A. Soldatov, “Elliptic Flow in Heavy-Ion Collisions at Energies $\sqrt{s_{NN}} = 2.7\text{-}39$ GeV,” Phys. Rev. C **91**, no.2, 024914 (2015) [arXiv:1401.2265 [nucl-th]].
- [25] A. D. Panagiotou, “ Λ^0 Nonpolarization: Possible Signature of Quark Matter,” Phys. Rev. C **33**, 1999-2002 (1986).
- [26] A. Ayala, E. Cuautle, G. Herrera and L. M. Montano, “ Λ^0 polarization as a probe for production of deconfined matter in ultrarelativistic heavy ion collisions,” Phys. Rev. C **65**, 024902 (2002) [arXiv:nucl-th/0110027 [nucl-th]].
- [27] R. Bellwied [E896], “Transverse polarization of Lambda hyperons in relativistic Au - Au collisions at the AGS,” Acta Phys. Hung. A **15**, 437-444 (2002).
- [28] K. Okubo [STAR], “Measurement of global polarization of Λ hyperons in Au+Au $\sqrt{s_{NN}} = 7.2$ GeV fixed target collisions at RHIC-STAR experiment,” EPJ Web Conf. **259**, 06003 (2022) [arXiv:2108.10012 [nucl-ex]].
- [29] M. S. Abdallah *et al.* [STAR], “Global Λ -hyperon polarization in Au+Au collisions at $\sqrt{s_{NN}}=3$ GeV,” Phys. Rev. C **104**, no.6, L061901 (2021) [arXiv:2108.00044 [nucl-ex]].
- [30] J. R. Adams [STAR], “Differential measurements of Λ polarization in Au+Au collisions and a search for the magnetic field by STAR,” Nucl. Phys. A **1005**, 121864 (2021)
- [31] E. Nazarova, R. Akhat, M. Baznat, O. Teryaev and A. Zinchenko, “Monte Carlo Study of Λ Polarization at MPD,” Phys. Part. Nucl. Lett. **18** (2021) no.4, 429-438.
- [32] G. Aad *et al.* [ATLAS], “Measurement of the transverse polarization of Λ and $\bar{\Lambda}$ hyperons produced in proton-proton collisions at $\sqrt{s} = 7$ TeV using the ATLAS detector,” Phys. Rev. D **91**, no.3, 032004 (2015) [arXiv:1412.1692 [hep-ex]].
- [33] <http://ckp.nrcki.ru/>